

JUPITER: STRUCTURE AND COMPOSITION OF THE UPPER ATMOSPHERE

S. K. ATREYA, T. M. DONAHUE, AND M. C. FESTOU

Department of Atmospheric and Oceanic Science, Space Physics Research Laboratory, University of Michigan

Received 1980 September 2; accepted 1981 March 12

ABSTRACT

The *Voyager* ultraviolet stellar occultation data yield a temperature of 200 ± 50 K at about 400 km, and the solar occultation data give 1100 ± 200 K at 1450 km above the ammonia cloud tops. The temperature gradient between 400 and 1450 km is approximately 1 K km^{-1} . The mesospheric temperature structure gives no strong indication of an Earth-like mesopause. The heating of the upper atmosphere appears to result from a combination of magnetospheric charged particle precipitation, ion drag, inertia gravity waves, and solar EUV. The volume mixing ratios of CH_4 and C_2H_6 at 325 km are measured to be $2.5(+3, -2) \times 10^{-5}$ and $2.5(+2.0, -1.5) \times 10^{-6}$, respectively, which are lower than in the stratosphere. The C_2H_2 volume mixing ratio is $\leq 5 \times 10^{-6}$ at 300 km. The homopause value of the equatorial eddy diffusion coefficient is found to be $1\text{--}2 \times 10^6 \text{ cm}^2 \text{ s}^{-1}$.

Subject headings: planets: atmospheres — planets: Jupiter

I. INTRODUCTION

The *Voyager 1* ultraviolet spectrometer (UVS) experiment of solar occultation provided the first measurement of the neutral temperature in the exosphere of Jupiter. The UVS α Leo stellar occultation data yielded thermal structure and altitude profiles of H_2 , CH_4 , C_2H_6 , and C_2H_2 in the mesosphere and thermosphere. On combining the UVS results with those from the *Voyager* infrared (IRIS), radio science (RSS), and imaging (ISS) data, we have arrived at the first measured height distributions of temperature and many photochemically active species in the atmosphere of Jupiter. This *Letter* is principally a discussion of the aeronomical implications of the upper atmospheric results.

II. EXPERIMENTAL RESULTS

We shall provide here only those details of the observations and data analysis which are pertinent to the theoretical discussion presented in this *Letter*.

Figure 1 shows both density and temperature profiles which have been obtained by means of the α Leo ultraviolet occultation experiment and other experiments on board the two *Voyager* spacecraft. The details of data reduction and analysis are presented elsewhere (Festou *et al.* 1981).

The temperature profile above 380 km is obtained by computing the absorption produced by molecular hydrogen in the Lyman and Werner bands below 1200 Å for various atmospheric profiles and comparing it to the absorption detected in the α Leo experiment. The temperature is found to be 200 ± 50 K at 430 \pm 50 km above the NH_3 cloud tops which are located at 600 mb level, $T = 150$ K. To reconcile the exospheric temperature and density provided by the solar occultation experiment (Atreya *et al.* 1979) with the lower altitude results of the stellar occultation experiment, it is necessary to increase the temperature almost

linearly with altitude between 430 and 1400 km. The lapse rate of about -1 K km^{-1} is found to give the best fit to the above two sets of data—both of which are for the tropics. It should be noted that further analysis of the solar occultation data, which take into account effects of short wavelength scattering in the instrument, have lowered the Atreya *et al.* (1979) exospheric temperature to 1100 ± 200 K. The RSS and IRIS data yield pressure-temperature combinations from 600 mb to about the 1 mb level, the α Leo UVS data provide density-temperature combinations in the $P < 1 \mu\text{b}$ ($z > 380$ km) region. The former give $T \approx 170$ K at $n \approx 4 \times 10^{16} \text{ cm}^{-3}$ (~ 1 mb), while the latter give $T \approx 200 \pm 50$ K at $n \approx 3 \times 10^{13} \text{ cm}^{-3}$ ($1 \mu\text{b}$). An assumption of linear change of temperature over the gap (1 mb to $1 \mu\text{b}$) can then be used for relating the α Leo data to the NH_3 cloud tops height reference, as has already been done in Figure 1. Although a negative temperature gradient between 1 mb and $1 \mu\text{b}$ cannot be entirely ruled out, early stellar occultations (see review by Hunten 1976) in the visible have suggested temperatures between $10 \mu\text{b}$ and 1 mb, similar to the ones we show by interpolation in Figure 1. The hydrocarbon data presented in this *Letter* further preclude temperatures too far removed from the 170–200 K range in the $5 \mu\text{b}$ to 1 mb range (see § III).

The hydrocarbon density profiles are obtained by studying the absorption characteristics of the stellar light in the 1200–1600 Å wavelength interval of the α Leo data. The analysis yields the volume mixing ratios of $\text{CH}_4 = 2.5(+3, -2) \times 10^{-5}$ and $\text{C}_2\text{H}_6 = 2.5(+2.0, -1.5) \times 10^{-6}$ at 325 km ($\sim 5 \mu\text{b}$). The upper limit for the C_2H_2 volume mixing ratio at 300 km is found to be 5×10^{-6} . C_2H_4 was not detected at these altitudes. The stratospheric volume mixing ratios for CH_4 , C_2H_6 , and C_2H_2 are $(1.4 \pm 0.45) \times 10^{-3}$, 5×10^{-6} , and 3×10^{-8} to 10^{-7} , respectively, from the IRIS data. There seems to be no inconsistency between the stratosphere and upper atmosphere mixing ratios of

the hydrocarbons since photolysis entirely alters their abundances at higher elevations. The helium density shown in Figure 1 is a representation of the IRIS measurement of its volume mixing ratio of 0.10 ± 0.03 (Hanel *et al.* 1979; D. Gautier 1980, personal communication).

III. DISCUSSION

The temperature from the NH_3 cloud tops (600 mb, 150 K) to the 1 mb level has been determined from the ground-based and *Voyager* IRIS and RSS measurements. The visible stellar occultation data give $T = 170 \pm 30$ K at $10 \mu\text{b}$ (Hunten 1976; Hunten and Veverka 1976) and perhaps a similar temperature up to the 1 mb level. We have found that a linear gradient of temperature between 1 mb (170 K) and $1 \mu\text{b}$ (200 K) would be physically more realistic for reconciling the CH_4 mixing ratio at $5 \mu\text{b}$ to its higher value in the stratosphere. A significant mesopause is not expected to develop.

No information on the neutral temperature in the $P < 10 \mu\text{b}$ region was available prior to the *Voyager* observations. The *Pioneer* radio science measurements of the electron density profiles indicated a warm plasma with a scale height corresponding to a plasma temperature of approximately 850 K (Fjeldbo *et al.* 1976; Hunten 1976). The *Voyager* RSS measurements confirmed the earlier *Pioneer* measurements but found

relatively higher plasma temperatures, on the order of 1200–1300 K. Theoretical considerations involving energy loss of the electrons and ions in the upper atmosphere led Henry and McElroy (1969) and Nagy *et al.* (1976) to conclude for both cold (150 K) and hot (1000 K) exospheres that there should be virtually no disequilibrium between the electron, ion, and neutral temperatures in the upper atmosphere. The first measurement of the neutral temperature in the upper atmosphere resulted from a solar occultation experiment carried out by *Voyager 1* UVS (Broadfoot *et al.* 1979). The analysis of the data yielded a temperature of 1450 ± 250 K, nearly 1500–2000 km above the NH_3 cloud tops (Atreya *et al.* 1979). As mentioned earlier, further analysis of the solar occultation data yields a somewhat lower exospheric temperature, but definitely in the 1000–1300 K range. The neutral temperature in the upper atmosphere is found to be in close agreement with the plasma temperature, as expected.

The important aeronomical question regarding the observed thermal structure is the mechanism by which heat is deposited in the upper atmosphere. Prior to the availability of the *Voyager 2* stellar occultation data, numerous ideas about the upper atmospheric energetics were in vogue. Based on the suspected vertical propagation of the inertia gravity waves in the β Sco data on the Jovian thermal structure (Elliot *et al.* 1974), French and Gierasch (1974) calculated an

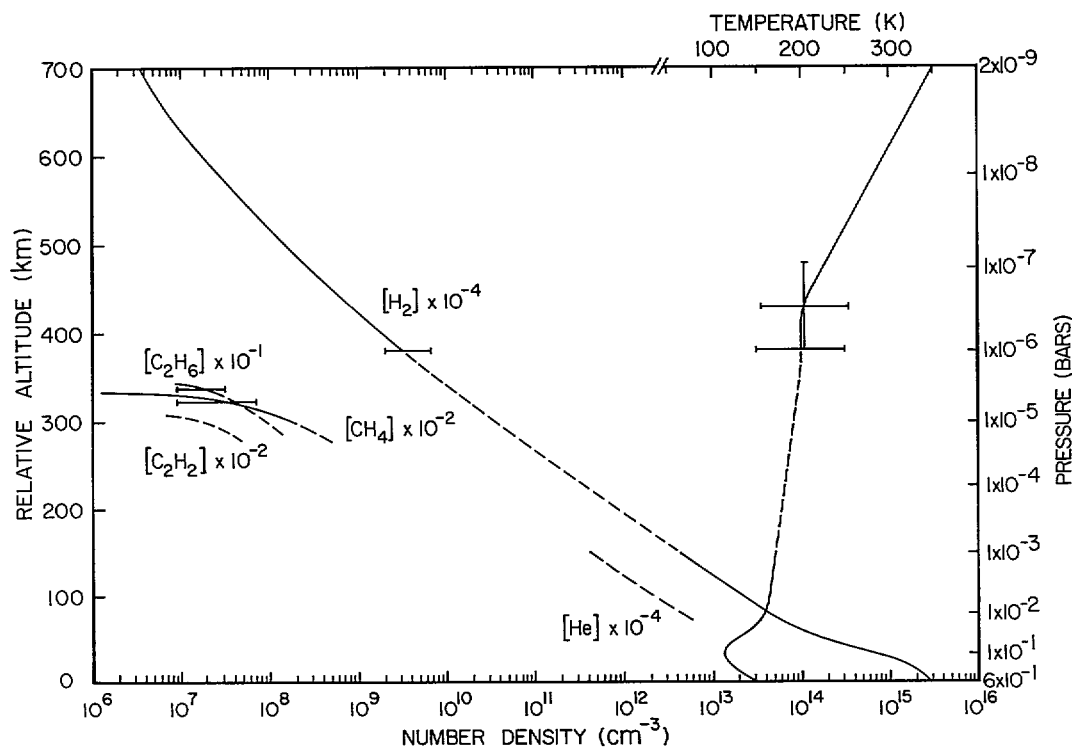


FIG. 1.— H_2 , CH_4 , C_2H_6 , and C_2H_2 density profiles, as well as the neutral temperature structure derived from the analysis of the α Leo occultation experiment. C_2H_2 density is an upper limit. The average temperature gradient is 1 K km^{-1} between 400 and 1450 km. All altitudes are relative to the NH_3 cloud tops located at $P = 600 \text{ mb}$, $T = 150 \text{ K}$. Pressures on the right ordinate correspond to the altitudes on the left ordinate. The broken line in the temperature profile shows extrapolations to the IRIS and RSS measurements.

energy flux of about $3 \text{ ergs cm}^{-2} \text{ s}^{-1}$ associated with these waves. Assuming that the waves dissipate their energy 5–10 scale heights above the homopause, Atreya and Donahue (1976) and Atreya *et al.* (1979) calculated that the above energy flux was more than adequate for raising the upper atmospheric temperature to 1000 K. It is not known, however, at what altitude the waves actually break up, or whether their energy is available as heat or they are merely reflected. The *Voyager* thermal data shown in Figure 1, however, rule out inertia gravity wave phenomena—whose evidence was also seen in the imaging data (Hunt and Muller 1979)—as the primary source for the upper atmospheric heating, even if the gravity waves dissipated their energy as heat, since it would result in a much greater temperature gradient above the homopause than has been observed.

Hunten and Dessler (1977) proposed an alternate mechanism in which penetration of the magnetospheric electrons would be responsible for heating of the neutral gas; no knowledge of the energy spectrum or energization mechanism of the incoming electrons was or is available. It should be remarked that the observed dayside intensity of $2.8 \pm 1.0 \text{ kR}$ in the H_2 Lyman and Werner band emissions (Shemansky *et al.* 1981) implies a soft electron energy flux of $\sim 0.3 \text{ ergs cm}^{-2} \text{ s}^{-1}$, which is significant only if it is deposited well above the homopause. The absence of the nightside H_2 -band emission and the presence of a small Ly α nightglow, on the other hand, imply a nighttime flux of soft energy electrons on the order of $0.04 \text{ ergs cm}^{-2} \text{ s}^{-1}$ (McConnell, Sandel, and Broadfoot 1980a). The soft electron penetration hypothesis is further complicated because it fails to explain satisfactorily, in a unified manner, the observed diurnal changes in the Ly α airglow and the Ly α equatorial bulge (Broadfoot *et al.* 1981; Sandel, Broadfoot, and Strobel 1980; Dessler, Sandel, and Atreya 1981). It is difficult to imagine a planet-wide precipitation of 50–100 eV soft electrons, particularly in the equatorial region for which the high thermospheric temperature has been measured. The same difficulty arises if one assumes that the heating may be caused by the transport of heavier ions or atoms from the Io-plasma torus; moreover, their densities are expected to be quite meager.

The *Voyager* UVS observations of the polar aurora on Jupiter indicate that a large amount of energy would be deposited in the region magnetically mapped by the Io-plasma torus (Thorne and Tsurutani 1979; Broadfoot *et al.* 1981). If this energy were to be spread evenly over the entire planet, it would amount to an energy flux of $0.2 \text{ ergs cm}^{-2} \text{ s}^{-1}$. (The electron energy input of $1.7 \times 10^{14} \text{ W}$ implied by the observed auroral intensities in Sandel *et al.* [1979] is incorrect and must be revised downward to $1.3 \times 10^{13} \text{ W}$.) The magnitude of this energy is quite tempting to use as a basis for supplying some heat to the thermosphere. The questions remain, however, about the altitude where this energy would be deposited and how efficiently the circulation from pole to equator would redistribute the energy. The equatorial region is not found to be much colder than the polar region, as is evident from the

plasma scale heights for the two regions (Eshleman *et al.* 1979a, b).

The high-energy auroral particles (MeV to keV) are expected to deposit their energy quite deep in the atmosphere. Indeed, the local temperature at about 700 km approaches 1600 K, as is evident from the *Voyager* 2 high-latitude plasma scale-height measurements (Eshleman *et al.* 1979b). The equatorial data (this Letter) do not, however, support this idea of a large temperature gradient at such depths.

Another possibility is the heating caused by the drag between the ions and the neutrals, or Joule heating. For Joule heating to be effective, our calculations indicate that the differential wind between the ions and neutrals of nearly 200 m s^{-1} at atmospheric density level of 10^{12} – 10^{14} cm^{-3} is required. The Joule heating mechanism is quite efficient in the sporadic E-type layers, such as those observed in the *Pioneer* data of the ionosphere and also suspected in the *Voyager* data (V. Eshleman 1979, personal communication). Should the Joule heating occur primarily in this region, it would almost necessarily result in a high temperature and a large lapse rate deep in the atmosphere, unlike the observations. On the other hand, one can imagine a scenario where the Joule heating mechanism would operate in the main ionosphere with maximum heating near the electron peak. The difficulty with such an idea is that the H_2 density at those levels is quite low for the required amount of heating. Because of the unavailability of the pertinent upper atmospheric dynamics data, it can only be said that Joule heating is of potential importance for the Jovian upper atmospheric energetics.

Next we turn to the question of the eddy diffusion coefficient, K . According to a theory developed by Hunten (1969) and Wallace and Hunten (1973), the eddy diffusion coefficient at the homopause, K_h , has an inverse functional dependence on the atomic hydrogen column abundance above the methane absorption layer, hence on the Jovian Ly α albedo. Based on this theory, one obtains K_h on the order of $(3 \pm 1) \times 10^8 \text{ cm}^2 \text{ s}^{-1}$ for the time of the *Pioneer* Jupiter observations (Ly $\alpha \approx 0.4 \text{ kR}$; Carlson and Judge 1974) and somewhat less than $10^6 \text{ cm}^2 \text{ s}^{-1}$ for the *Voyager* epoch (Ly $\alpha \approx 14 \text{ kR}$). There is, however, considerable uncertainty about the mechanism for the production of atomic hydrogen, particularly during the time of the *Voyager* Jupiter observations when the solar activity and the exospheric temperature were quite high. With $K_h \approx 10^6 \text{ cm}^2 \text{ s}^{-1}$, photodissociation and dissociative photoionization of H_2 and photolysis of CH_4 and NH_3 cannot produce the required amount of atomic hydrogen; the excess atomic hydrogen must be supplied by some other source such as particle dissociation of H_2 . In view of these complications in the atomic hydrogen production, the Wallace and Hunten relationship can be used to arrive at only an order of magnitude estimate of K_h for the *Voyager* epoch.

The analysis of the Jovian He 584 Å airglow (McConnell, Sandel, and Broadfoot 1980b) observed by *Voyager* UVS yields $K_h = 8 \times 10^5 \text{ cm}^2 \text{ s}^{-1}$, $6 \times 10^6 \text{ cm}^2 \text{ s}^{-1}$, and $2 \times 10^7 \text{ cm}^2 \text{ s}^{-1}$, respectively, for temperatures of

150 K, 500 K, and 1000 K in the scattering region. The actual temperature in the scattering region is more like 200 K (this *Letter*), implying K_h of $1 \times 10^6 \text{ cm}^2 \text{ s}^{-1}$.

Interpretation of the electron density profiles measured by *Voyager 1* RSS yields $K_h \approx 1\text{--}3 \times 10^5 \text{ cm}^2 \text{ s}^{-1}$ (Atreya, Donahue, and Waite 1979). The deduction of K_h from the ionospheric data is indirect and depends on the assumptions of the ion production mechanism, and it should therefore be regarded as an order of magnitude estimate.

The α Leo stellar occultation data provide a more direct measure of the eddy diffusion coefficient at the homopause. The hydrocarbons would drop in density quite rapidly above the homopause because of their larger molecular weights than the background gas H_2 . The homopause, however, may be located somewhat higher than the level at which the heavier gases such as hydrocarbons could drop in density due to photolysis. We shall, therefore, assume the mathematical definition of the homopause, i.e., the level at which the eddy diffusion coefficient, K , equals the molecular diffusion coefficient, D .

We have examined, by solving the methane photochemistry, the relationship between the H_2 density at the height where a methane vertical optical depth, τ_{CH_4} , of unity at $\text{Ly}\alpha$ is reached and the value of the eddy diffusion coefficient at the homopause, K_h . $\text{Ly}\alpha$ wavelength is chosen since most of the methane photolysis takes place at this wavelength; therefore, it provides a more accurate level for comparison with the data. Photochemical analysis for the hydrocarbons is relevant for the equatorial region where particle destruction and subsequent alteration of the density profiles is highly improbable. It should be noted that the densities of all hydrocarbons drop off sharply within 1 or 2 scale heights of each other. Photolysis calculations were performed according to the chemical scheme discussed in Strobel (1975) and its improvement described in Yung and Strobel (1980). The calculations were done for numerous cases with tropopause values of the eddy diffusion coefficient, K_0 , of 1×10^2 , 5×10^2 , 1×10^3 , 5×10^3 , 1×10^4 , and $5 \times 10^4 \text{ cm}^2 \text{ s}^{-1}$, and assuming $M^{-1/2}$ and M^{-1} variations of K with height, M being the atmospheric number density. In order to reproduce the observed characteristics of the hydrocarbons, including the region of the falloff in their densities, we required $1 \times 10^3 \text{ cm}^2 \text{ s}^{-1} > K_0 > 5 \times 10^2 \text{ cm}^2 \text{ s}^{-1}$ and $\bar{K} \propto M^{-1/2}$ (approximate) variation. The theoretical behavior between the H_2 density, at the level where $\tau_{\text{CH}_4} = 1$, and K_h is shown in Figure 2. The CH_4 density profile deduced from the α Leo data (Fig. 1) gives the H_2 density, at the height where τ_{CH_4} of unity is reached, to be $5.5(+3.5, -1.5) \times 10^{14} \text{ cm}^{-3}$ or at 285(+10, -15) km. The range includes the total statistical uncertainty in the determination of the H_2 and CH_4 densities. Referring to Figure 2, the H_2 density of $5.5(+3.5, -1.5) \times 10^{14} \text{ cm}^{-3}$ corresponds to $K_h = 1.4(+0.8, -0.7) \times 10^6 \text{ cm}^2 \text{ s}^{-1}$ at the homopause in the tropics. This result is compatible with an

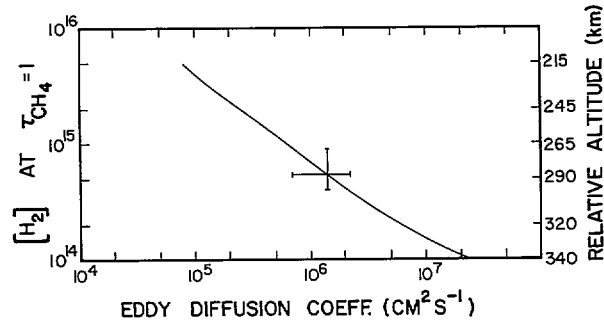


FIG. 2.— H_2 density at the height where the methane vertical optical depth of unity at $\text{Ly}\alpha$ is reached vs. the eddy diffusion coefficient at the homopause. The right ordinate shows the relative altitudes corresponding to the densities on the left ordinate. The statistical uncertainty in K_h , shown by the horizontal bar, corresponds to the statistical uncertainty in the determination of the height of $\tau_{\text{CH}_4} = 1$, represented by the vertical bar in the H_2 density.

indirect inference of $K = 1 \times 10^6 \text{ cm}^2 \text{ s}^{-1}$, based on the He 584 Å airglow data. We also note a large decrease—by as much as a factor of 100—in K_h from the *Pioneer* epoch to the *Voyager* encounter. Such a drastic change in the value of the eddy mixing term is indicative of large temporal variations in the convective patterns of the Jovian atmosphere, perhaps related to the solar activity.

The IRIS measurements yield a He molar fraction of 0.10 ± 0.03 (Hanel *et al.* 1979; D. Gautier 1980, personal communication), a value consistent with the solar composition ratio of He/ H_2 , implying almost definitely that the internal heat source of Jupiter is due to the release of accretion energy.

The question of atomic hydrogen distribution remains a puzzle. The $\text{Ly}\alpha$ observations can place upper limits on the column abundance of hydrogen above the methane absorption layer. Its value turns out to be $\sim 1 \times 10^{17} \text{ cm}^{-2}$ (McConnell, Sandel, and Broadfoot 1980a), if resonance scattering of the solar $\text{Ly}\alpha$ is the sole mechanism responsible for the observed Jovian $\text{Ly}\alpha$ intensity. The number increases to about $3 \times 10^{17} \text{ cm}^{-2}$ in the region where a bulge in the intensity of $\text{Ly}\alpha$ has been detected (Sandel, Broadfoot, and Strobel 1980). The excess atomic hydrogen in the bulge is proposed to be related directly to a longitudinal asymmetry in the flux of precipitating high energy electrons, which is a consequence of the corotating magnetospheric convection (Dessler, Sandel, and Atreya 1981). Whatever the atomic hydrogen height distribution on Jupiter may be, it is expected to be strongly governed by the spectrum of the charged particles incident on top of the atmosphere. Consequently, atomic hydrogen is expected to show large latitudinal and temporal variations.

This research was sponsored by a grant from the Planetary Atmospheres Program of the NASA Solar System Exploration Division.

REFERENCES

- Atreya, S. K., and Donahue, T. M. 1976, in *Jupiter*, ed. T. Gehrels (Tucson: University of Arizona Press), pp. 304-318.
- Atreya, S. K., Donahue, T. M., Sandel, B. R., Broadfoot, A. L., and Smith, G. R. 1979, *Geophys. Res. Letters*, **6**, 795-798.
- Atreya, S. K., Donahue, T. M., and Waite, J. H., Jr. 1979, *Nature*, **280**, 795-796.
- Broadfoot, A. L. *et al.* 1979, *Science*, **204**, 979-982.
- Broadfoot, A. L. *et al.* 1981, *J. Geophys. Res.*, in press.
- Carlson, R. W., and Judge, D. L. 1974, *J. Geophys. Res.*, **19**, 3623.
- Dessler, A. J., Sandel, B. R., and Atreya, S. K. 1981, *Planet. Space Sci.*, **29**, 215-224.
- Elliot, J. L., Wasserman, L. H., Veverka, J., Sagan, C., and Liller, W. 1974, *Ap. J.*, **190**, 719-729.
- Eshleman, V. R., Tyler, G. L., Wood, G. E., Lindal, G. F., Anderson, J. D., Levy, G. S., and Croft, T. A. 1979a, *Science*, **204**, 976.
- . 1979b, *Science*, **206**, 959-962 (also see n. 11).
- Festou, M. C., Atreya, S. K., Donahue, T. M., Sandel, B. R., Shemansky, D. E., and Broadfoot, A. L. 1981, *J. Geophys. Res.*, in press.
- Fjeldbo, G., Kliore, A., Seidel, B., Sweetnam, D., and Woiceshyn, P. 1976, in *Jupiter*, ed. T. Gehrels (Tucson: University of Arizona Press), pp. 238-245.
- French, R. G., and Gierasch, P. J. 1974, *J. Atmos. Sci.*, **31**, 1707-1712.
- Hanel, R. A. *et al.* 1979, *Science*, **204**, 972-976.
- Henry, R. J. W., and McElroy, M. B. 1969, *J. Atmos. Sci.*, **26**, 912.
- Hunt, G. E., and Muller, J. P. 1979, *Nature*, **280**, 778-780.
- Hunten, D. M. 1969, *J. Atmos. Sci.*, **26**, 826-834.
- . 1976, in *Jupiter*, ed. T. Gehrels (Tucson: University of Arizona Press), pp. 22-31.
- Hunten, D. M., and Dessler, A. J. 1977, *Planet. Space Sci.*, **25**, 817-821.
- Hunten, D. M., and Veverka, J. 1976, in *Jupiter*, ed. T. Gehrels (Tucson: University of Arizona Press), p. 247.
- McConnell, J. C., Sandel, B. R., and Broadfoot, A. L. 1980a, *Icarus*, **43**, 128-142.
- . 1980b, *Planet. Space Sci.*, in press.
- Nagy, A. F., Chameides, W. L., Chen, R. H., and Atreya, S. K. 1976, *J. Geophys. Res.*, **81**, 5567-5569.
- Sandel, B. R., Broadfoot, A. L., and Strobel, D. F. 1980, *Geophys. Res. Letters*, **7**, 508.
- Sandel, B. R. *et al.* 1979, *Science*, **206**, 962-966.
- Shemansky, D. E., McConnell, J. C., Sandel, B. R., and Broadfoot, A. L. 1981, preprint.
- Strobel, D. F. 1975, *Rev. Geophys. Space Phys.*, **13**, 372-382.
- Thorne, R. M., and Tsurutani, B. R. 1979, *Geophys. Res. Letters*, **6**, 649.
- Wallace, L., and Hunten, D. M. 1973, *Ap. J.*, **182**, 1013-1031.
- Yung, Y. L., and Strobel, D. F. 1980, *Ap. J.*, **239**, 395.

S. K. ATREYA, T. M. DONAHUE, and M. C. FESTOU: Department of Atmospheric and Oceanic Science, Space Physics Research Laboratory, University of Michigan, Ann Arbor, MI 48109

